CHAPTER VII

A STUDY OF THE DIELECTRIC RELAXATION IN SOME NEMATIC LIQUID CRYSTALS USING THE FREEDERICKSZ TRANSITION TECHNIQUE

Introduction

Distortions induced in a nematic liquid crystal by electric fields are more complicated than those induced by magnetic fields because in the former case the internal field is not in general in the same direction as the applied field. In addition, the dielectric constants of the medium are also frequency dependent in general. For polar molecules, there is always a Debye relaxation of the orientation polarisation. As a consequence, when an alternating electric field is used, the critical voltage corresponding to Freedericksz transition becomes frequency dependent in the vicinity of the relaxation frequency.

In the isotropic phase of a polar compound, the Debye relaxation frequency occurs in the giga hertz region. The reason for this is straight forward. The torque due to the applied field on the dipole tending to orient the molecule is countered by a

frictional torque. The Debye relaxation time is given by (Debye 1945)

$$\tau_0 = \frac{\xi}{2k_B T} \qquad (7.1)$$

where ξ is a frictional constant. The relaxation frequency (f_R) is then $\sim \frac{1}{\tau}$. Above this frequency the dipole moment can no longer take part in the polarisation of the medium and hence the entire polarisation arises from the induced polarisation and $\varepsilon \sim n^2$.

In a nematic medium, we have two dielectric constants — $\varepsilon_{\parallel}$ along the director and $\varepsilon_{\perp}$ normal to the director. When a nematic liquid crystal is subjected to an alternating field, these two dielectric constants exhibit quite different frequency dependences. Maier and Meier (1961) observed that both $\varepsilon_{\parallel}$ and $\varepsilon_{\perp}$ exhibit the normal Debye dipole dispersion like a normal polar liquid in the giga hertz range but $\varepsilon_{\parallel}$ exhibits an additional dispersion at fairly low frequencies - in the radio frequency region. They pointed out that this additional dispersion is due to an orientational relaxation of the long axis component of the permanent electric dipole. Meier and Saupe (1966) interpreted this in terms of the 180° rotation of the molecule about its short axis.

The alignment of the long axis component (μ_L) of the permanent dipole moment by the electric field is hindered by a potential barrier due to the intermolecular forces in the nematic phase. Assuming that μ_L can orient itself only by a rotation of the entire molecule, Meier and Saupe (1966) extended the Debye theory of dipole relaxation to include the nematic potential. The nematic potential is characterised by a potential barrier q. This leads to a retardation factor g by which the relaxation time τ_o is enhanced. The relevant expressions were derived by them on a simplified model,

$$\tau_R = g\,\tau_o \qquad (7.2)$$

where τ_o is given by equation (7.1), and

$$g = \frac{k_B T}{q}\left[\exp\left(\frac{q}{k_B T}\right) - 1\right] \qquad (7.3)$$

q can, in principle, be derived from a molecular statistical theory of the nematic phase (Maier and Saupe 1958, 1959, 1960).

Recently Martin et al. (1971) have derived these quantities using a more detailed theory. Since the temperature variation of ξ can be represented to a good approximation as

$$\xi = \xi_0 \exp(-\frac{q_{visc}}{k_B T}) \qquad (7.4)$$

and

$$f_R \propto \exp - [\frac{q_{nem} + q_{visc}}{k_B T}] \qquad (7.5)$$

Therefore f_R should show a strong temperature dependence, decreasing as the temperature is lowered.

The usual method of studying the dielectric relaxation is to measure the capacitance of a nematic liquid crystal cell with appropriate molecular alignment. We have used our set up of determining elastic constants to study the dielectric relaxation in a few compounds.

The deformations induced by an electric field have *bean* studied by Gruler and Meier (1972) and Deuling (1972). In addition, Deuling et al. (1974) have studied the problem of crossed electric and magnetic fields with magnetic field as a stabilising field. We shall now consider a case of a magnetic field applied normal to the undistorted director in the presence of a stabilising alternating electric field.

Freedericksz transition with crossed $\vec{E}$ and $\vec{H}$

Consider a homeotropically aligned nematic

liquid crystal contained between two plane conducting glass plates. A magnetic field is applied in the plane of the sample film (figure 7.1). We choose the coordinate system such that the undistorted $\vec{n}$ is along X–axis and the magnetic field along Z–axis.

Let $\vec{E}$ be the electric field applied along X axis and $\vec{H}$ be the magnetic field so that a weak distortion takes place *in* the medium. At any point, let θ be the angle made by the local director with X axis, θ varies along X only. Hence $\vec{n}$ = (cos θ, 0, sin θ), $\vec{E}$ = (E,0,0), $\vec{H}$ = (0, 0, H). The equation for the free energy density can be written as

$$W = \frac{1}{2}k_{11}(\nabla \cdot \vec{n})^2 + \frac{1}{2}k_{33}(\vec{n} \times \nabla \times \vec{n})^2 - \frac{1}{2}\vec{E} \cdot \vec{D} - \frac{1}{2}\Delta\chi(\vec{H} \cdot \vec{n})^2 \qquad (7.6)$$

where $\vec{D}$ is the electric displacement vector.

We assume that $\nabla \cdot \vec{D} = 0$ and $\nabla \times \vec{E} = 0$. Minimising the energy of the medium (similar to that shown in Chapter I) we get the following expression for k_{33}

$$k_{33} = \frac{\Delta\chi\, x_o^2\, H_e^2}{\pi^2} - \frac{\Delta\varepsilon\, V^2}{\pi^2} \qquad (7.7)$$

where H_e is the critical field and $\Delta\varepsilon = \varepsilon_{\parallel} - \varepsilon_{\perp}$.

$V = E \cdot x_o$ the voltage applied.

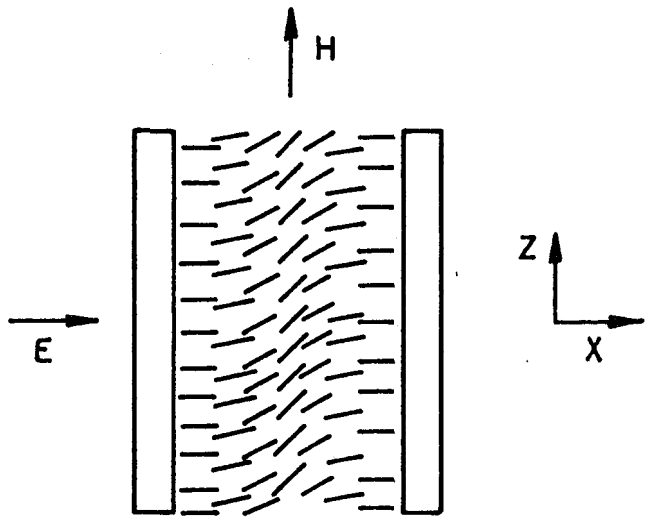

Chapter 7.1

Schematic diagram of the geometry used to study the effect of crossed electric and magnetic fields.

From equation (7.7) we see that at any temperature and frequency of the electric field, H_e^2 increases linearly with V^2.

In the absence of any electric field, let H_o be the critical magnetic field, then

$$k_{33} = \frac{\Delta\chi\, x_o^2\, H_o^2}{\pi^2} \qquad (7.8)$$

Pros equations (7.7) and (7.8) we can get an expression for the anisotropy sf dielectric constant

$$\Delta\varepsilon = \Delta\chi\, x_o^2 \left(\frac{H_e^2 - H_o^2}{V^2}\right) \qquad (7.9)$$

or

$$\Delta\varepsilon \propto \frac{H_e^2 - H_o^2}{V^2} \qquad (7.10)$$

at any temperature.

As the frequency of the applied voltage Is increased and approaches the relaxation frequency, $c_,$ decreases and hence the taw $\{(H_e^2 - H_o^2)/V^2\}$ decreases.

Now if we consider the usual k_{11} geometry (Chapter I) with electric field as the deforming field

$$k_{11} = \frac{\Delta\varepsilon \cdot V_o^2}{\pi^2} \qquad (7.11)$$

Hence at any temperature

$$\Delta\epsilon \propto \frac{1}{V_c^2} \qquad (7.12)$$

Again as the relaxation frequency approaches, V_c starts increasing.

Hence one expects to be able to study the dielectric relaxation in the two geometries using equations (7.10) and (7.12). However as Gruler (1974) has pointed out, in the case of nematic liquid crystals having molecules possessing shape anisotropy (pear or banana shaped), k_{11} and k_{33} themselves exhibit frequency dependences. He concluded that k_{11} should show a low frequency relaxation (like $\epsilon_{//}$) while k_{33} a high frequency relaxation (like $\epsilon_{\perp}$).

We can understand the relaxation of k_{11} and k_{33} physically as follows: Consider pear shaped molecules with permanent dipole moments along its length (figure 7.2). In the absence of any external field, the molecules arrange themselves in such a way as to compensate their shape anisotropy (figure 7.2a). If a splay is induced in the medium by an external field (say an AC electric field), in one half of the cycle the dipole moment tend to align along $\vec{E}$ in such a way as to favour the shape anisotropy (figure 7.2b). In the other half of the cycle, the dipoles have to

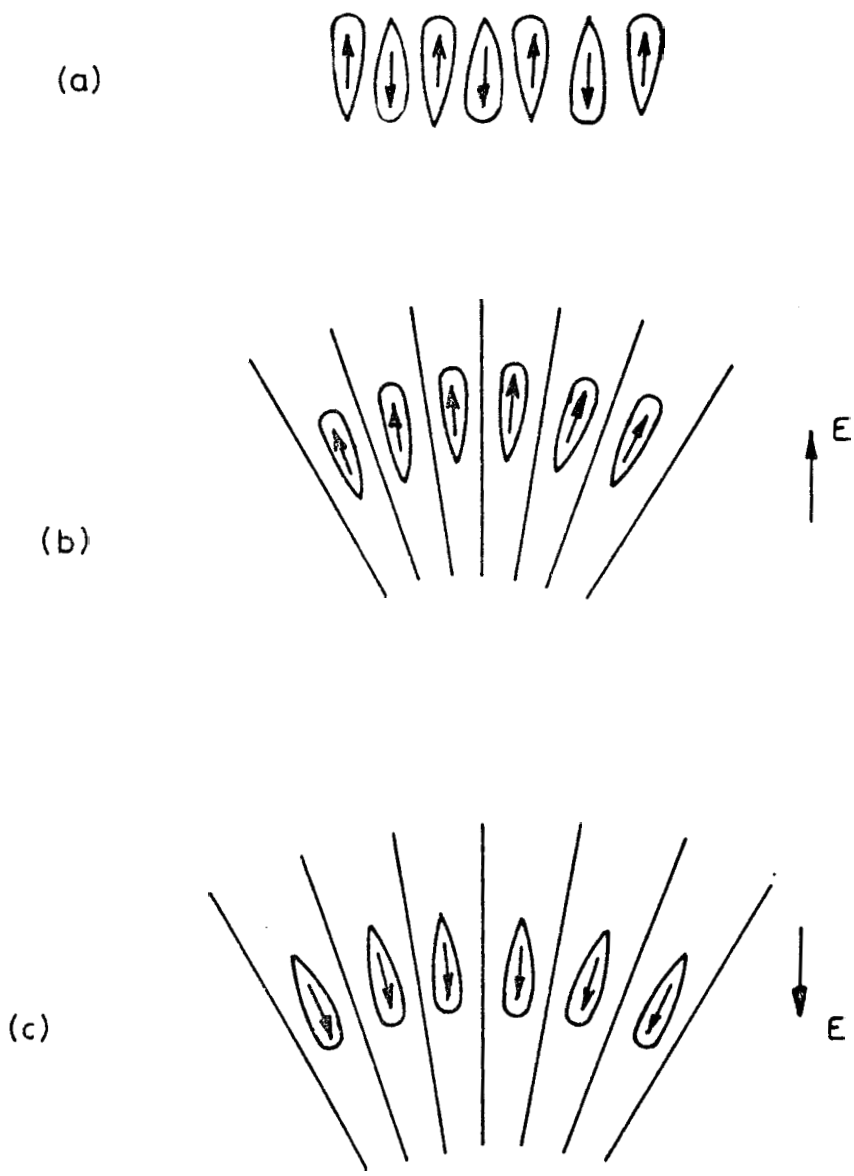

Figure 7.2

(a) The alignment of molecules having shape anisotropy in the absence of external electric or magnetic fields.
(b & c) The molecular alignment during the two halves of one cycle of the alternating electric field in a deformed sample.

align against the splay (figure 7.2c), since the director field itself is not able to follow the external electric field.

Hence in rotating about the short axis, the molecules have to not only work against the nematic potential barrier but also the barrier due to the shape anisotropy. However Deuling (1574) has shown that this effect does not alter the critical field for Freedericksz transition, as in this case the deformation is negligibly small. Hence in our experiments we do not expect to observe the relaxation of k_{11} and we attribute the measured frequency dependence to be entirely due to the dipolar relaxation.

EXPERIMENTAL

The erst up for crossed electric and magnetic fields is similar to the one used for the determination of k_{33}(Chapter III) excepting that, in the present case tin oxide coated glass plates were used. The electric contacts for the glass plates were given by means of platinum foils. The homeotropic alignment was obtained by treating the glass plates with cetyl tetramethyl ammonium bromide.

For k_{11} geometry, tho homogeneous alignment was obtained by vacuum depositing silicon at an oblique angle.

Results and discussions

In the k_{33} geometry we have measured the critical magnetic field H_c as a function of the stabilising voltage (V) for a fixed temperature and frequency. As expected from equation (7.7), a plot of H_c^2 re. V^2 is a straight line. Figure 7.3 includes the values for 6CB and 8 OCB. The values are given in Table 7.1.

In the case of 6CB we have plotted $(\frac{H_c^2 - H_o^2}{V^2})$ and V_c^2 as functions of frequency at $T_{NI} - T = 4°C$ (figure 7.4). The values are given in Table 7.2. The molecular structure of 6CB is shown in figure 7.5. In this case the C≡N end group is the only polar group (leaving out the C-H bonds), and is practically collinear with the molecular long axis. Hence we expect a simple relaxation process and the dielectric anisotropy decreases considerably at f_R attaining a small value for $f > f_R$.

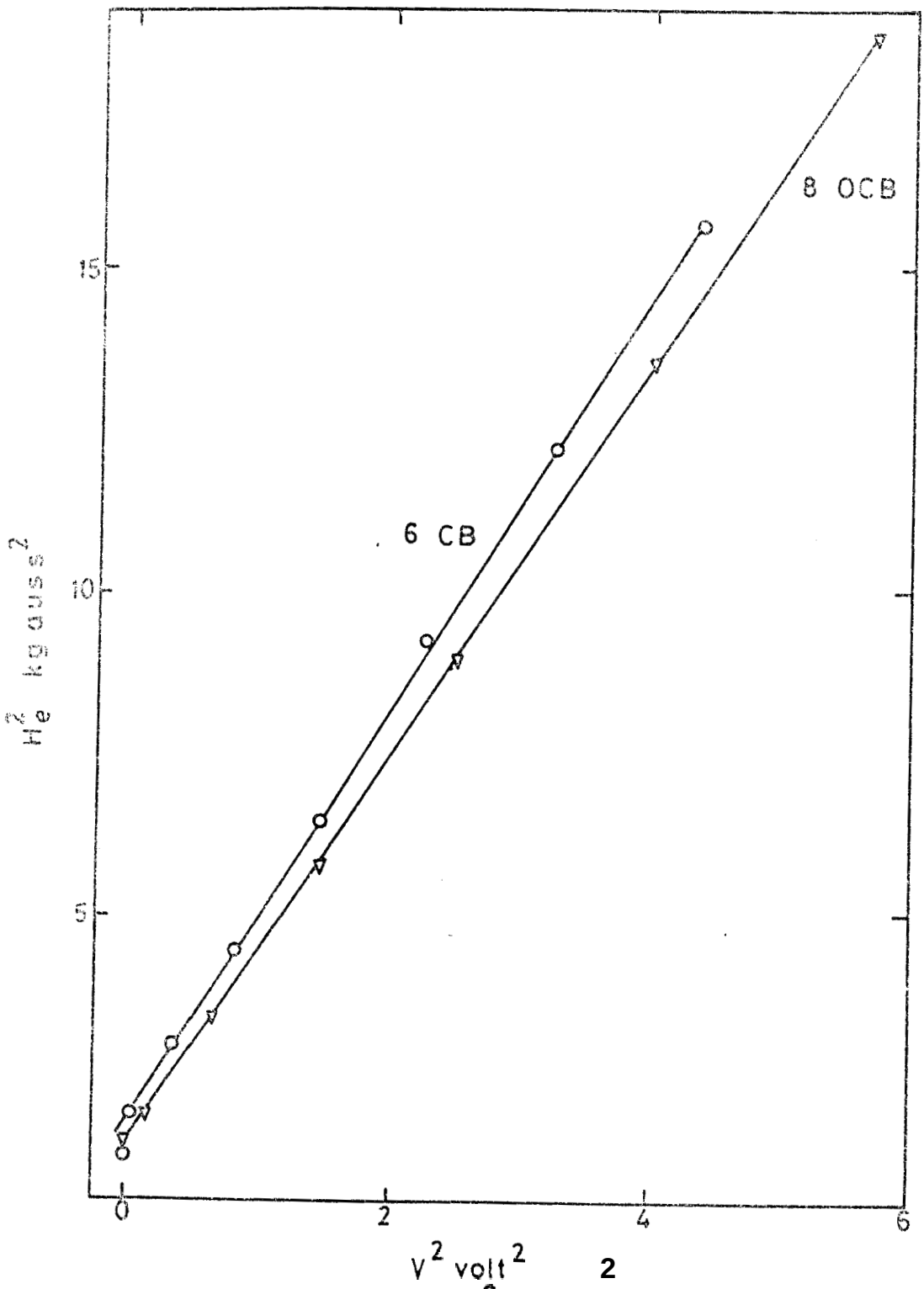

Figure 7.3: The plot of H_e^2 vs. V^2 where H_e is the critical magnetic field when a stabilizing voltage V is applied across the sample. The frequency is 0.5 MHz. Sample thickness ~ 50 μm; circles: 6CB (T_{NI}-T=4°C) and triangles: 8 OCB (T_{NI}-T=12°C).

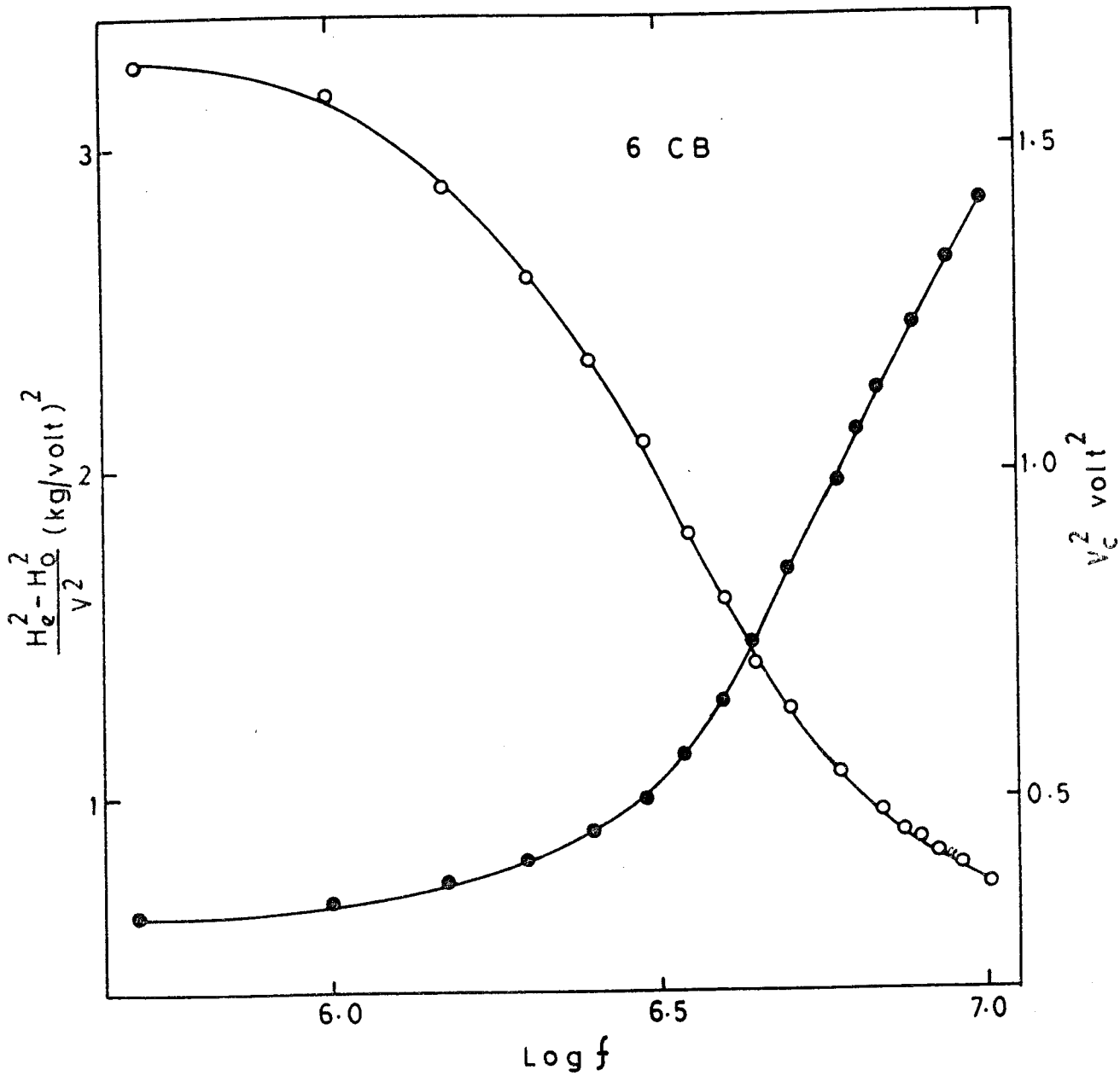

Figure 7.4

The plots of $[(H_e^2-H_o^2)/V^2]$ (open circles) and V_c^2 (filled circles) as functions of frequency in the case of 6CB. Sample thickness $\sim$ 50 μm (k_{33} geometry) and $\sim$ 120 μm (k_{11} geometry) $T_{NI} - T = 4°C$.

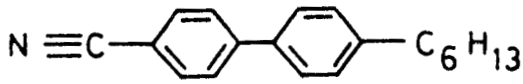

6 CB

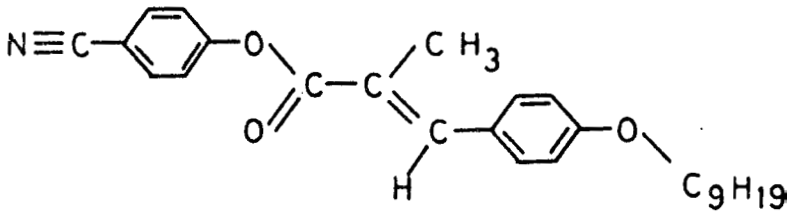

9 OMCPC

Figure 7.5

Molecular structures of 6CB and 9 OMCPC

For 9 OMCPC, the plot of $(\frac{H_e^2 - H_o^2}{V^2})$ and V_c^2 as functions of frequency for three different temperatures *ore* shown in figure 7.6. The values axe tabulated in Table 7.3.

From equation (7.11), we have $V_c^2 \propto \frac{k_{11}}{\Delta\varepsilon}$. Since $k_{11} \propto S^2$, it follows that $\Delta\varepsilon \propto S$. Thus at low frequencies ($<< f_R$), V_c^2 increases with decreasing temperature (figure 7.6). At the same frequency, one would expect that $(\frac{H_e^2 - H_o^2}{V^2})$ which is proportional to $\Delta\varepsilon$ to remain independent of temperature ($\Delta\chi \propto S$). However experimentally we see (figure 7.6) that $\frac{\Delta\varepsilon}{\Delta\chi}$ has a tendency *to* increase at lower temperatures.

From the curves of $(\frac{H_e^2 - H_c^2}{V^2})$, we see that beyond

continued ..

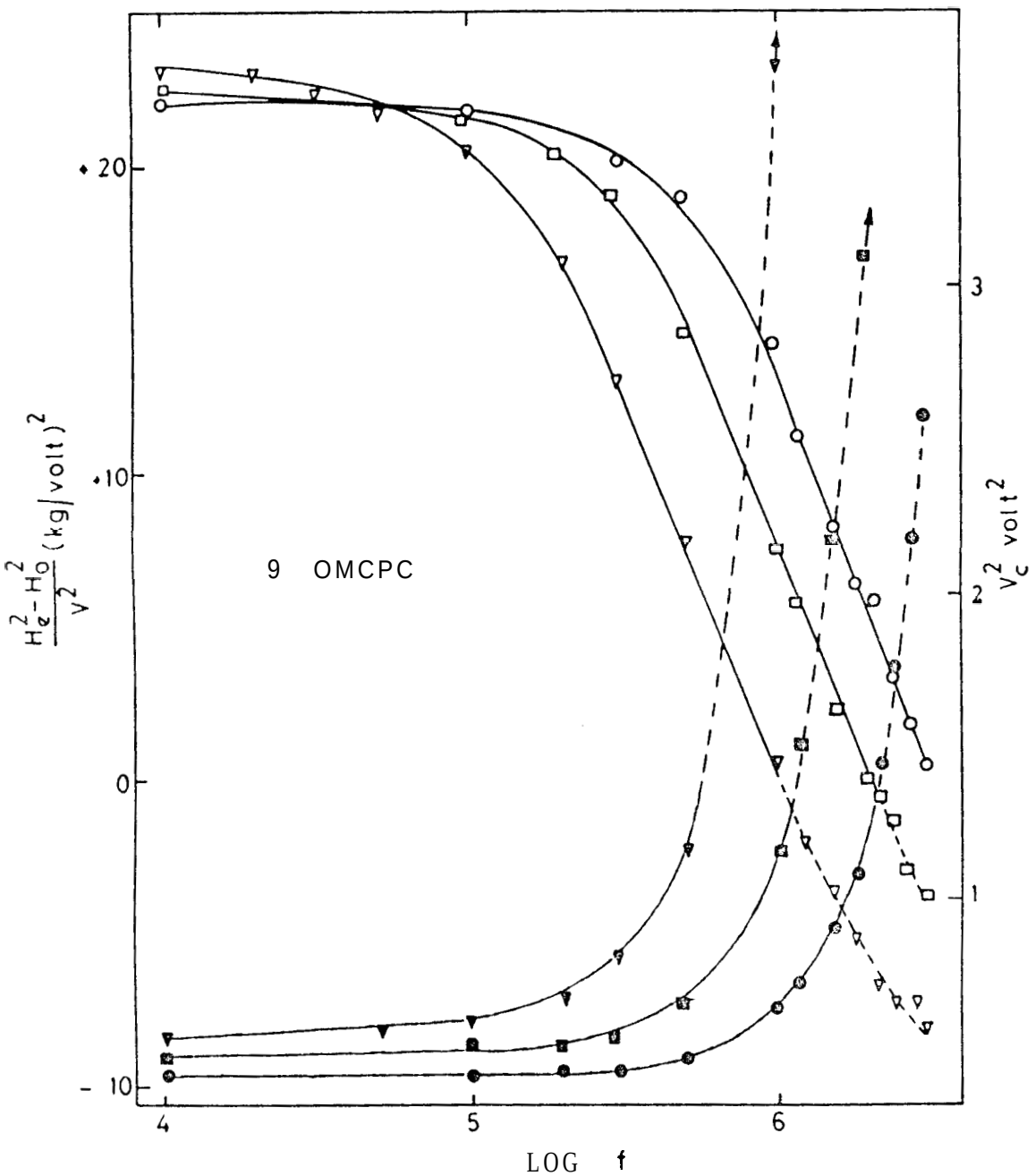

Figure 7.6

The plots of $(H_e^2-H_o^2)/V^2$ (open symbols) and V_c^2 (filled symbols) as functions of frequency. $T_{NI}-T$ = 4°C (circles), 10°C (squares), 16°C (triangles). (Sample thickness ~ 25 μm).

a certain frequency f_o, depending upon the temperature, H_e becomes less than H_o. This means that $\Delta\epsilon$ has changed sign at this frequency. Or in other words, beyond f_o the sample behaves as a negative dielectric anisotropy material. With the decrease in temperature f_o decreases. We might mention here that a reversal of $\Delta\epsilon$ has been observed in some other compounds as well as mixtures by earlier workers (see for example De Jeu and Lathouwers 1974, Klingbich et al. 1975, Bauer et al. 1973, Bata et al. 1974).

9 OMOPC has a complicated molecular structure (figure 7.5). There is an alkoxy end group which has components both parallel and perpendicular to the long axis. The $\overset{O}{\overset{\|}{C}} - O$ group essentially exhibits a long axis component and perhaps a weak normal component. In addition we have the strong $C \equiv N$ dipole again practically along the long axis. Hence one can expect a fairly complicated relaxation in this compound. In particular, we can expect that beyond a frequency f_o the perpendicular component to predominate the dielectric property giving rise to a negative dielectric anisotropy.

From equation (7.5) we see that a plot of log f_R vs. $1/T$ should be a straight line, the slope being a

measure of the total activation energy $Q = q_{nem} + q_{visc}$. de Jeu and Lathouwers (1974) have demonstrated that the calculated activation energy does not change if f_R La replaced by f_o in equation (7.5). Moreover, since f_o should be close to f_R, we can for *our* present purposes identify f_o with f_R. In figure 7.7 we hare plotted log f_R vs. 1/T. The calculated value of $Q \simeq 1$ eV.

The sign reversal of $\Delta\epsilon$ in this case leads to certain interesting results. In tho k_{11} *pone%*— as we approach f_o, we observe the electrohydrodynamic patterns in the field of view (figure *7.8).* It is interesting to note that these Williams-domain like pattern is characterised by a domain width which is of the order of sample thickness. In fact there have been some earlier observations of this kind of instability at much lower frequencies (de Jeu et al. 1973, Rondelez 1975). Goosens (1972) has developed a theory *for* this effect which occurs at frequencies much higher than the charge relaxation frequency (typically $\sim$ 1 KHz in the cases with the usual conductivities). by noting the formal similarity between the dielectric loss which occurs in the neighbourhood of the relaxation frequency and the conductivity in the sample. In fact, if is well known that the conduction regime of

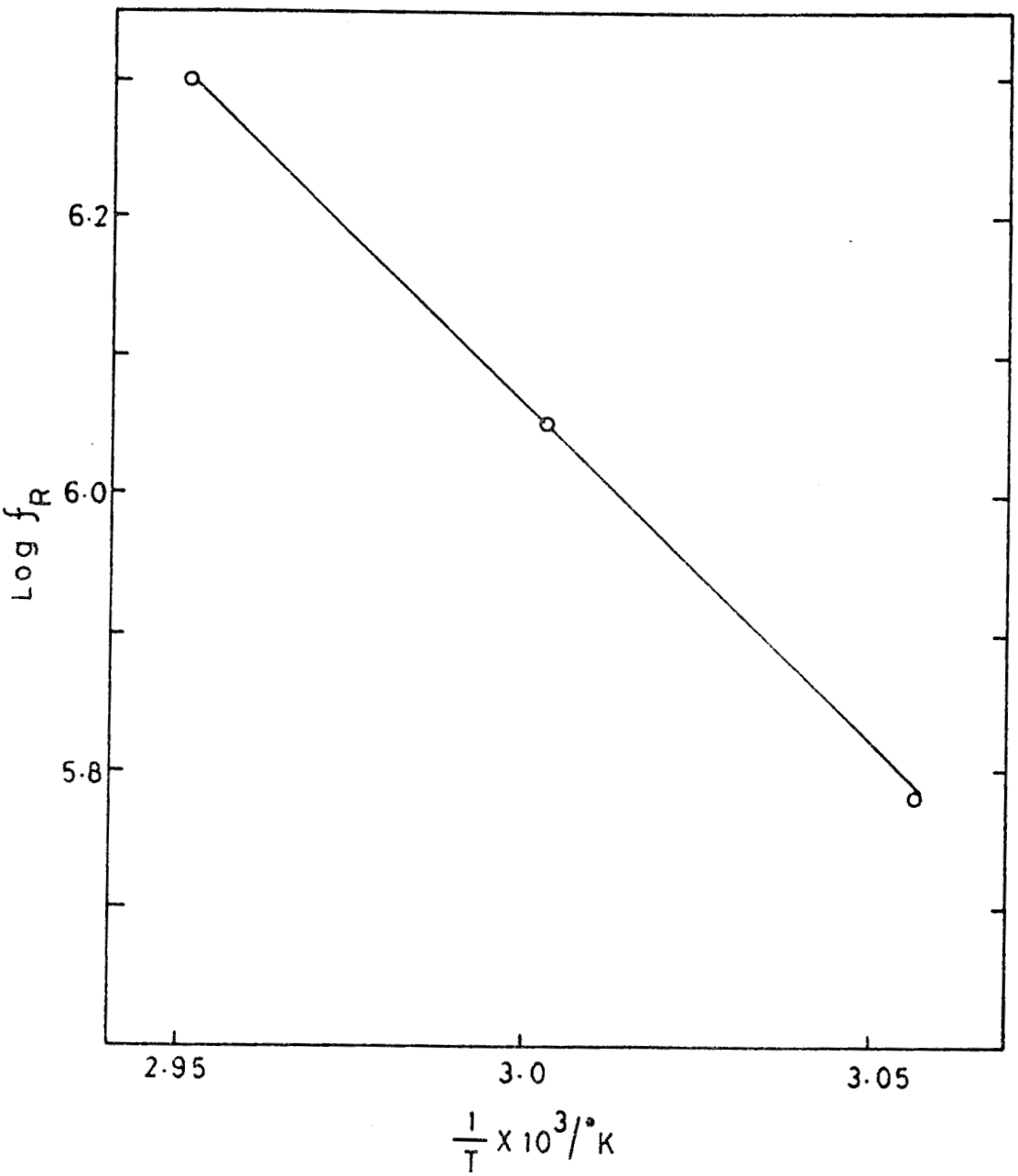

Figure 7.7

Logarithmic plot of relaxation frequency f_R versus the inverse of absolute temperature T for 9 OMCPC.

Figure 7.8

(a) Inversion walls seen in the homogeneously aligned sample of 9 OMCPC when electric field (300 KHz) is increased beyond the critical value. The sample thickness is 10 μm and the voltage applied is 0.65 V. (b) The pattern seen when the frequency is increased to 1 MHz. The voltage applied is 0.95 V. The photograph shows the superposition of inversion walls and electrohydrodynamic patterns. (c) The pattern seen when the frequency is raised to 3 MHz. Voltage applied is 4V.

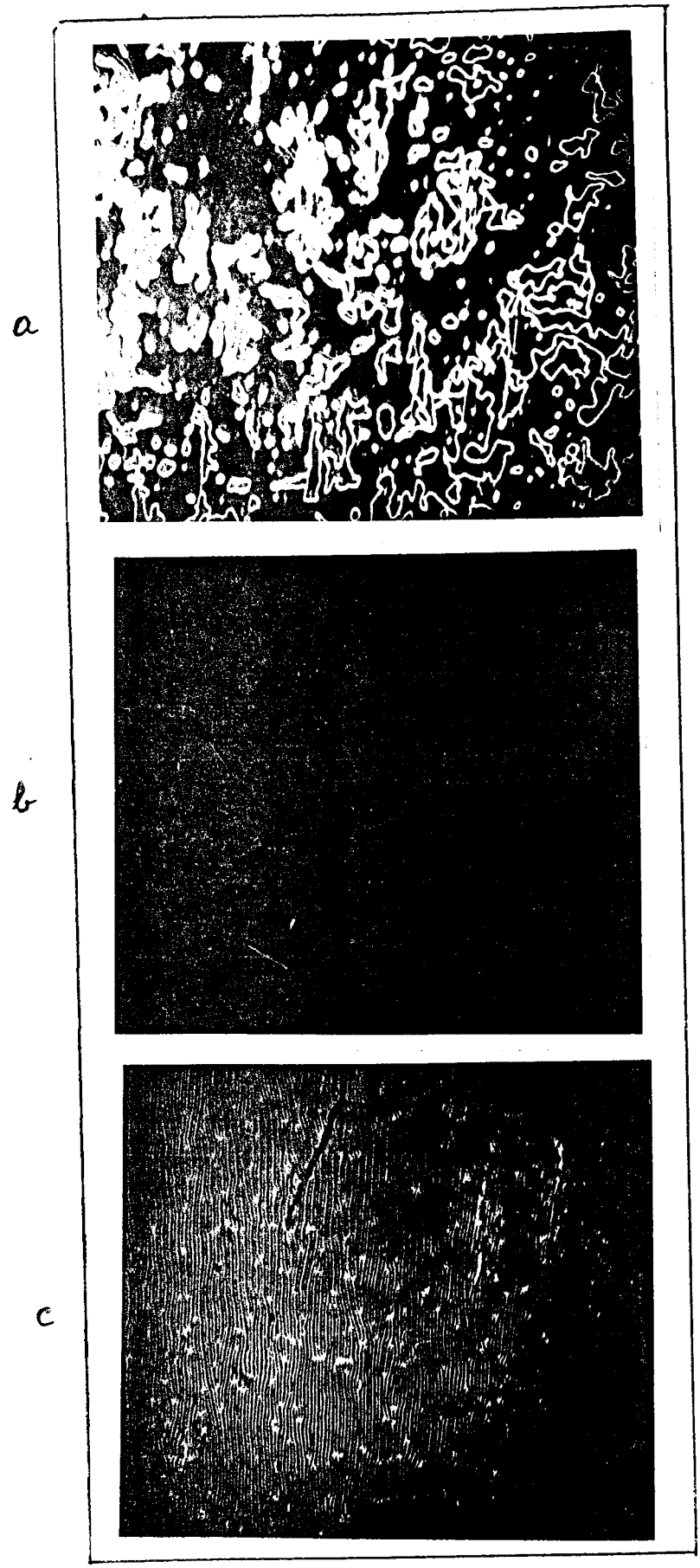

a

b

c

electrohydrodynamic instabilities can occur for both weakly positive as well as negative dielectric anisotropy materials. Hence in the present case we have shown $\frac{H_e^2 - H_o^2}{V^2}$ and V_c^2 beyond f_o by dotted lines.

It is possible that in this region the electrohydrodynamic instabilities influence strongly the observed threshold fields.

de data and Lathouwers (1974) have identified a conduction regime near the f_o of some mixtures. They observed dynamic scattering at voltages somewhat larger than the threshold voltage (V_{th}) for the appearance of domains. Further, V_{th} was found to increase as the frequency was increased above f_o, and beyond a second frequency limit f_c, chevrons were also observed.

More recently, Smith et al. (1975) have pointed lout that even under excitation at high frequencies the domain size of the flow pattern will *be* comparable to the thickness of the sample under a few different conditions. (a) Even if the medium has a low negative dielectric anisotropy, in the high frequency range, the ionic diffusion currents become important for $f \geq 10$ KHz. Taking this effect into account Smith

et al. (1975) have shown that the width of the domains (λ) is approximately equal to the thickness of the sample x_o even in the dielectric regime in which the curvature oscillates in phase with the applied field, by contrast with the conduction regime in which the charge density oscillates (see also Dubois Violette et al. 1971). (The effect of the ionic diffusion has not been taken into account in Goosen's theory.); (b) When $\Delta\varepsilon$ is weakly positive, again there will be effectively a conduction regime at high frequencies characterised by $\lambda \simeq x_o$.

Our observations can hence be understood in terms of these explanations. However the observations reported here cannot distinguish the various possible mechanisms, and it is difficult to say which of these is the one responsible for these instabilities.

References

Bata, L., Haranadh, C. and Molnar, G. 1974 KFKI Reports 55.

Baur, G., Stieb, A. and Meier, G. 1973 Liquid Crystals and Ordered Fluids, Ed. Johnson, J.F. and Porter, R.S., Vol. 2, p. 645.

Debye, P. 1945 'Polar Molecules' p.83, Dover Publications

De Jeu, W.H., Gerritsma, C.J., Van Zanten, P. and Goossens, W.J.A. 1972 . 39A. 355.

De Jeu, W.H. and Lathouwers, Th.W. 1974 Mol. Cryst. Liquid Cryst. 26, 225.

Deuling, H.J. 1972 Mol.Cryst.Liquid Cryst. 19, 123.

Deuling, H.J., Guyon, E. and Pieranski, P. 1974 Solid State Commun. 15, 277.

Deuling, H.J. 1974 Solid State Commun. 14, 1073.

Dubois Violette, E., de Gennes, P.G. and Parodi, O. 1971 J. de Phys. 32, 305.

Goossens, W.J.A. 1972 Phys. Lett. 40A, 95.

Gruler, H. and Meier, G. 1972 Mol.Cryst.Liquid Cryst. 16, 299.

Gruler, H. 1974 J. Chem. Phys. 61, 5408.

Klingbich, R.T., Genova, D.J. and Bucher, H.K. 1975 Mol.Cryst.Liquid Cryst. 27, 1.

Maier, W. and Saupe, A. 1958 Z. Naturforsch. 13a, 564

Maier, W. and Saupe, A. 1959 Z.Naturforsch. 14a, 882.

Warier, W. and Saupe, A. 1960 Z.Naturforsch. 15a, 287.

Maier, W. and Meier, G. 1961 Z.Naturforsch. 16a, 470.

Maier, W. and Meier, G. 1961 Z.Naturforsch. 16a, 1200.

Martin, A.J., Meier, G. and Saupe, A. 1971 Symp. Faraday Soc. Liquid Crystals No.5, p. 119.

Meier, G. and Saupe, A. 1966 Mol. Cryst. 1, 515.

Rondelez, F. 1975 (private communication).

Smith, I.W., Galerne, Y., Legerwall, S.T., Dubois Violette, E. and Durand, G. 1975 J. de Phys. , C1-237.

Table 7.1

Variation of threshold field H_e with the applied Voltage V.

(i) 6 CB $T_{NI}-T = 4°C$ $f = 0.5$ MHz

V^2	H_e^2
0	1.21
0.09	1.85
0.35	2.89
0.81	4.41
1.44	6.45
2.25	9.24
3.24	12.25
4.41	15.60

(ii) 8 OCB $T_{NI}-T = 12°C$ $f = 0.5$ MHz

V^2	H_e^2
0	1.38
0.15	1.90
0.64	3.35
1.44	5.66
2.53	8.88
4.00	13.47
5.71	18.58

Table 7.2

Dielectric relaxation in 6CB

V = 2 Volts, $T_{NI}-T = 4°C$,

H_c = 1.1 Kgauss

Frequency (MHz)	$\frac{H_e^2 - H_c^2}{V^2}$ $(Kg/Volt)^2$	V_c^2
0.5	3.25	0.32
1	3.17	0.34
1.5	2.87	0.37
2.0	2.59	0.40
2.5	2.35	0.45
3.0	2.09	0.50
3.5	1.81	0.56
4.0	1.60	0.64
4.5	1.40	0.74
5.0	1.26	0.85
6.0	1.07	0.98
6.5	1.00	1.06
7.0	0.96	1.12
8.0	0.88	1.23
9.0	0.79	1.32
10.0	0.76	1.42

Table 7.3

Dielectric relaxation in 9 OMCPC

(i) $T_{NI}-T=4°C$, V=0.5 volt, H_o = 3.41 Kgauss

freq. (Hz)	$\frac{H_e^2-H_o^2}{V^2}\times10^{-6}$ (Kgauss/Volt)^2	V_o^2 volt^2
1 K	22.0	0.44
10 a	22.0	0.44
300 K	22.0	0.44
200 K	20.7	0.45
$500 K	20.1	0.46
500 K	19.1	0.49
1 M	14.3	0.64
1.2 M	11.2	0.74
1.5 M	8.5	0.92
1.8 M	6.5	1.10
2.1 M	5.9	1.46
2.4 M	3.3	1.77
2.7 M	1.9	2.19
3.0 a	0.5	2.59

(ii) $T_{NI}-T=10°C$, V=0.48 Volt, H_o=3.71 Kgauss

freq. Hz	$\frac{H_e^2-H_o^2}{V^2}\times10^{-6}$ (Kgauss/Volt)^2	V_o^2 volt^2
1 K	22.4	0.51
10 K	22.4	0.51
50 K	22.4	0.51
100 K	21.6	0.52
200 K	20.5	0.53
300 K	19.0	0.56
500 K	14.7	0.67
1 M	7.6	1.17
1.2 M	5.3	1.51
1.5 M	2.3	2.19
1.8 M	0	3.10
2.1 M	-0.6	4.33
2.4 M	-1.3	5.90
2.7 M	-2.9	8.00
3.0 M	-3.8	10.30

(iii) $T_{NI}-T=16°C$, V=0.5 Volts, H_o=3.78 Kgauss

1 K	23.8	0.57
10 K	23.1	0.57
20 K	23.1	0.57
30 K	22.4	0.57
50 K	21.7	0.58
100 K	20.6	0.61
200 K	16.8	0.68
300 K	13.1	0.81
500 K	7.8	1.17
1 M	0.6	3.72
1.2 M	-2.1	5.57
1.5 M	-3.6	10.00
1.8 M	-5.3	16.08
2.1 M	4.7	28.20
2.4 M	-7.3	41.10
2.7 M	-7.3	53.40
3.0 M	-8.2	63.36